



UNIVERSITY
OF TRENTO

DIPARTIMENTO DI INGEGNERIA E SCIENZA DELL'INFORMAZIONE

38123 Povo – Trento (Italy), Via Sommarive 14
<http://www.disi.unitn.it>

ANALYSIS OF THE POTENTIALITIES AND LIMITATIONS OF
THE INTEGRATION BETWEEN THE IMSA AND THE LEVEL SET
METHOD FOR INVERSE SCATTERING

M. Benedetti, D. Lesselier, M. Lambert, and A. Massa

January 2011

Technical Report # DISI-11-243

ANALYSIS OF THE POTENTIALITIES AND LIMITATIONS OF THE INTEGRATION BETWEEN THE IMSA AND THE LEVEL SET METHOD FOR INVERSE SCATTERING

M. Benedetti⁽¹⁾⁽²⁾, D. Lesselier⁽²⁾, A. Massa⁽¹⁾, and M. Lambert⁽²⁾

⁽¹⁾*Department of Information and Communication Technologies, University of Trento, Via Sommarive 14, 38050 Trento, Italy, andrea.massa@ing.unitn.it, Web-page: www.eledia.ing.unitn.it*

⁽²⁾*Département de Recherche en Électromagnétisme - Laboratoire des Signaux et Systèmes, CNRS-SUPELEC-UPS 11, 3 rue Joliot-Curie, 91192 Gif-sur-Yvette CEDEX, France, lesselier@lss.supelec.fr; Web-page: www.lss.supelec.fr*

Abstract

In the framework of the inverse scattering methodologies, this paper is aimed at preliminarily assessing the integration between the Iterative Multi-Scaling Approach and the Level-Set-based method. In order to enhance the potentialities of the Level-Set-based minimization, a multi-resolution procedure is employed for allowing a finer discretization only in those regions of interest where the scatterers are located thus reducing the whole computational burden with respect to a single-resolution approach. In order to demonstrate the effectiveness of the IMSA Level Set technique, a set of representative numerical results are presented and discussed.

Key words: inverse scattering, multi-resolution technique, level set.

1. INTRODUCTION

The reconstruction of inaccessible scenarios by means of inverse scattering techniques is a challenging problem, because of the limited amount of information that can be collected in the scattering experiments and the ill-posedness of the inverse problem. Due to the band limited nature of the scattered field [1], a significant and independent set of data is not available and the necessary spatial resolution of the object under test can be obtained by means of the exploitation of the available a-priori information [2][3] or using effective iterative techniques.

To help with the solution, recent developments reported in the literature suggest to split the original problem into a series of successive sub-problems according to the general strategy of “divide and conquer”. Following these guidelines, this paper deals with the analysis of potentialities and limitations of the integration between a multi-resolution approach [4][9] and an effective minimization technique based on shape deformation [2][5][6]. The former is a multi-resolution strategy [called Iterative Multi-Scaling Approach (IMSA)] aimed at improving at each step of a multi-step procedure the resolution accuracy in a subset of the whole investigation domain. More in detail, starting from a “coarse” representation of the scatterer profile, the region of interest (RoI) is iteratively focused onto the area where the unknown scatterer is supposed to be located by processing the information about the dielectric distribution estimated at the previous step. As a consequence, the spatial resolution is improved only inside the RoIs, keeping in each sub-problem a lower ratio between problem unknowns and independent field samples thus reducing the the occurrence of the local minima [7][8].

At each step, the dielectric profile in the RoI is estimated through the Level-Set-based method. As a matter of fact, starting from the a-priori knowledge of the homogeneous scatterer under test, the shape is a sufficient parameter for the characterization of the unknown object therefore an effective Level Set representation can be profitably used.

2. MATHEMATICAL FORMULATION

Let us consider a cylindrical two-dimensional geometry where a set of V transverse-magnetic plane waves $E_{inc}^v(x, y)\hat{z}$ (with $v = 1, \dots, V$) at a fixed frequency f successively illuminates an investigation domain (D_I). An unknown homogeneous dielectric object with known relative permittivity ϵ_C and conductivity σ_C but unknown shape and position occupies

an area $\Upsilon \in D_I$. The background is an homogeneous and lossless medium with the electromagnetic properties of the vacuum ($\epsilon_0, \mu_0, \sigma = 0$). The region D_I is described by the object function $\tau(x, y)$ given by

$$\tau(x, y) = \begin{cases} \tau_C & (x, y) \in \Upsilon \\ \tau_B & \text{otherwise} \end{cases} \quad (1)$$

where $\tau_B = 0$ and $\tau_C = j2\pi f\epsilon_0(\epsilon_C - 1) - j\frac{\sigma_C}{2\pi f\epsilon_0}$ are the object functions of the background and of the object, respectively. Starting from the knowledge of the scattered field $E_{scatt}^v(x, y)\hat{z}$ collected in an observation domain D_O at $M(v)$ measurement points ($v = 1, \dots, V$) uniformly distributed on a circle of radius ρ and the incident field $E_{inc}^v(x, y)\hat{z}$ in D_I , the inverse scattering problem can be recast as the solution of the following integral equations

$$\begin{aligned} E_{scatt}^v(\underline{r}) &= \\ &= j2\pi f\mu_0 \int_{D_I} \tau(\underline{r}') E_{tot}^v(\underline{r}') G_{2D}(\underline{r}, \underline{r}') d\underline{r}' \end{aligned} \quad (2)$$

$\underline{r} \in D_O$

$$\begin{aligned} E_{inc}^v(\underline{r}) &= E_{tot}^v(\underline{r}) - \\ &+ j2\pi f\mu_0 \int_{D_I} \tau(\underline{r}') E_{tot}^v(\underline{r}') G_{2D}(\underline{r}, \underline{r}') d\underline{r}' \end{aligned} \quad (3)$$

$\underline{r} \in D_I$

where G_{2D} is the 2D free-space Green's function, $\underline{r} = (x, y)$, and $E_{tot}^v(\underline{r}) = E_{inc}^v(\underline{r}) + E_{scatt}^v(\underline{r})$ is the total electric field.

Since a closed-form solution of the scattering equations (2) and (3) is not available, a suitable discretization of D_I has to be performed so as to get a numerical solution. Moreover, the information content of scattering data is limited [7]. Therefore, a multi-resolution strategy has to be considered in order to achieve a fine resolution of the unknown object, keeping a limited number of unknown and fully exploiting the limited amount of data.

Towards this end, the ‘‘Iterative Multi-Scaling Approach’’ (IMSA) is employed [4]. Such a strategy consists of a sequence of S steps (with $s = 1, \dots, S$) aimed at reconstructing the region of interest. More in detail, at the first step ($s = 1$) the region of interest $R_{(s=1)}$ corresponds to the area D_I . According to the method of moments, $R_{(s=1)}$ is discretized in N_{IMSA} sub-domains.

The s th region of interest is analyzed by means of the Level-Set-based technique [2]. To this end, at the first multi-resolution step (i.e., $s = 1$), a Level Set $\phi_{(s=1)}$ defined in $R_{(s=1)}$ is initialized according to an oriented distance function

$$\begin{aligned} \phi_{(s)}(\underline{r}_{n(s)}) &= \\ &= \begin{cases} -\min_{d(s)=1, \dots, D(s)} \{\rho_{n(s)d(s)}\} \\ \quad \text{if } \tau_0(\underline{r}_{n(s)}) = \tau_C \\ +\min_{d(s)=1, \dots, D(s)} \{\rho_{n(s)d(s)}\} \\ \quad \text{if } \tau_0(\underline{r}_{n(s)}) \neq \tau_C \end{cases} \end{aligned} \quad (4)$$

where $\rho_{n(s)d(s)}$ represents the distance between $\underline{r}_{n(s)} = (x_{n(s)}, y_{n(s)})$, being the center of the $n(s)$ th square cell with side $l_{(s)}$, and $\underline{r}_{d(s)}$, which is the d th border-cell ($d(s) = 1, \dots, D(s)$) of the initial trial solution τ_0 . Then, an iterative procedure is considered for minimizing through the evolution of $\phi_{(s)(k_s)}$ the following multi-resolution cost function

$$\Theta(\phi_{(s)(k_s)}) = \frac{\sum_{v=1}^V \left\| [E_{SM}^v] - \sum_{i=1}^{I_R} \Im \{ [\phi_{(i)(k_i)}] \} \right\|^2}{\sum_{v=1}^V \| [E_{SC}^v] \|^2} \quad (5)$$

where k_s is the iteration index in the s th step and $i = 1, \dots, I_R$. $I_R = s$ is the maximum or current resolution index.

In (5), $[E_{SM}^v]$ is a $M(v) \times 1$ array whose elements are $E_{SM}^v(\underline{r}_{m(v)})$ [$m(v) = 1, \dots, M(v)$] representing the measured data collected by the $m(v)$ th probe.

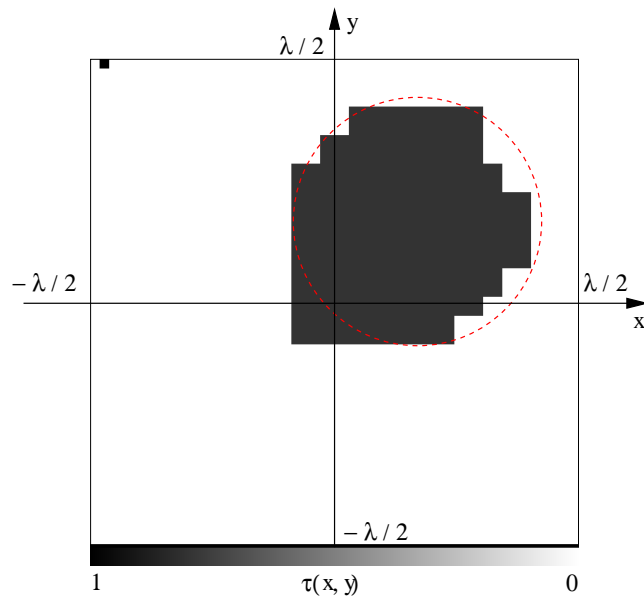


Figure 1. Choice of the optimal Δt . Reconstruction of a cylinder having radius $\lambda/2$ with $\Delta t = 0.01$.

$\mathfrak{F} \{ [\phi_{(i)(k_i)}] \}$ indicates the $M(v) \times 1$ vector of the computed scattered field $[E_{SC,(i)(k_i)}^v]$ which depends on the Level Set function $\phi_{(i)(k_i)}$ (according to the matrix representation, $[\phi_{(i)(k_i)}] = \{ \phi_{(i)(k_i)}(\underline{\mathbf{r}}_{n(i)}); n(i) = 1, \dots, N_{IMSA} \}$ is a $N_{IMSA} \times 1$ array).

The first stage of k_s th iteration at the step s is concerned with the computation of the electrical fields related to the trial solution $\tau_{(s)(k_s)}$. In particular, the array of the total electric field $[E_{tot,(s)(k_s)}^v] = \{ E_{tot}^v(\underline{\mathbf{r}}); \underline{\mathbf{r}} \in R_{(i)}, i = 1, \dots, I_R \}$ is computed through the operator $\chi \{ \cdot \}$

$$\begin{aligned} [E_{tot,(s)(k_s)}^v] &= \chi \{ [\Psi_{(i)(k_i)}] \} = \\ &= [E_{inc,(s)}^v] (1 - [G_{int,(s)}] \Lambda \{ [\Psi_{(i)(k_i)}] \})^{-1} \end{aligned} \quad (6)$$

where $\Lambda \{ \cdot \}$ returns the object function diagonal matrix $[\tau_{(s)(k_s)}]$, whose nonzero elements are $\{ \tau_{(s)(k_s)}(\underline{\mathbf{r}}); \underline{\mathbf{r}} \in R_{(i)}, i = 1, \dots, I_R \}$. More in detail, $[\tau_{(s)(k_s)}]$ is calculated using the multi-resolution expansion as follows

$$\begin{aligned} \tau_{(s)(k_s)}(\underline{\mathbf{r}}) &= \\ &= \sum_{i=1}^{I_R} \sum_{n(i)=1}^{N_{IMSA}} \tau_{(i)(k_i)}(\underline{\mathbf{r}}_{n(i)}) \end{aligned} \quad (7)$$

with

$$\begin{aligned} \tau_{(i)(k_i)}(\underline{\mathbf{r}}_{n(i)}) &= \\ &= \begin{cases} \tau_C & \text{if } \Psi_{(i)(k_i)}(\underline{\mathbf{r}}_{n(i)}) \leq 0 \\ 0 & \text{otherwise} \end{cases} \end{aligned} \quad (8)$$

and

$$\begin{aligned} \Psi_{(i)(k_i)}(\underline{\mathbf{r}}_{n(i)}) &= \\ &= \begin{cases} \phi_{(i)(k_i)}(\underline{\mathbf{r}}_{n(i)}) & \text{if } i = s \\ \phi_{(i)(k_{i,opt})}(\underline{\mathbf{r}}_{n(i)}) & \text{if } \begin{cases} i < s \\ \underline{\mathbf{r}}_{n(i)} \in R_{(i)} \end{cases} \end{cases} \end{aligned} \quad (9)$$

$k_{i,opt}$ being the last iteration of i th multi-resolution processes. In equation (6), $[G_{int,(s)}]$ is the internal Green's matrix at s th resolution level.

Thus, the scattered field is computed by means of the operator $\mathfrak{S}(\cdot)$ introduced in (5), which is defined as $\mathfrak{S} \{ [\phi_{(i)(k_i)}] \} = \{ E_{SC,(i)(k_i)}^v(\underline{r}_{m(v)}); m(v) = 1, \dots, M(v) \}$. $E_{SC,(i)(k_i)}^v(\underline{r}_{m(v)})$ is calculated through the solution of a direct problem starting from the total electric field $E_{tot,(i)(k_i)}^v(\underline{r}_{n(i)})$ and the contrast function $\tau_{(i)(k_i)}(\underline{r}_{n(i)})$, with $n(i) = 1, \dots, N_{IMSA}$. After $[E_{SC}^v] = \sum_{i=1}^{I_R} \mathfrak{S} \{ [\phi_{(i)(k_i)}] \}$ has been determined, the fitness value of $\phi_{(s)(k_s)}$ is evaluated using (5).

The second stage deals with the computation of the velocity $N_{IMSA} \times 1$ array $[\mathcal{V}_{(s)(k_s)}]$ in order to update the Level Set function $\phi_{(s)(k_s)}$ inside $R_{(s)}$. Following the guidelines suggested in [2], $[\mathcal{V}_{(s)(k_s)}]$ is calculated through the solution of an adjoint problem, which considers an electric field distribution given by $E_{SM}^v(\underline{r}_{m(v)}) - E_{SC,(s)(k_s)}^v(\underline{r}_{m(v)})$ in the $M(v)$ measurement points of D_O .

The last stage of the minimization procedure is concerned with the update of the Level Set through a numerical version of the Hamilton-Jacobi equation in order to get $\phi_{(s)(k_{s+1})}$.

Finally the iteration index is incremented ($k_s = k_s + 1$) and the iterative optimization is carried on until a stopping criterion is verified. More in detail, at each iteration k_s of the s th step, each value $\tau_{(s)(k_s)}(\underline{r}_{n(i)})$ of the current contrast function is compared with that in the same position at previous J_τ iterations. Each j th comparison ($j = 1, \dots, J_\tau$) returns a number of changed pixels $p_N^{(j)}$. If the numbers $p_N^{(j)}, \forall j$, are smaller than a fixed threshold γ_τ , the contrast function is considered as stationary. Moreover, the fitness function is stationary if the normalized error is lower than a fixed value $\gamma_\mathfrak{S}$ for $J_\mathfrak{S}$ iterations. The Level-Set-based minimization is stopped at the iteration k_{opt} when the stability conditions of both the fitness and contrast functions become true. Otherwise, a maximum number of iterations $k_{s,opt} = K_{max}$ is needed.

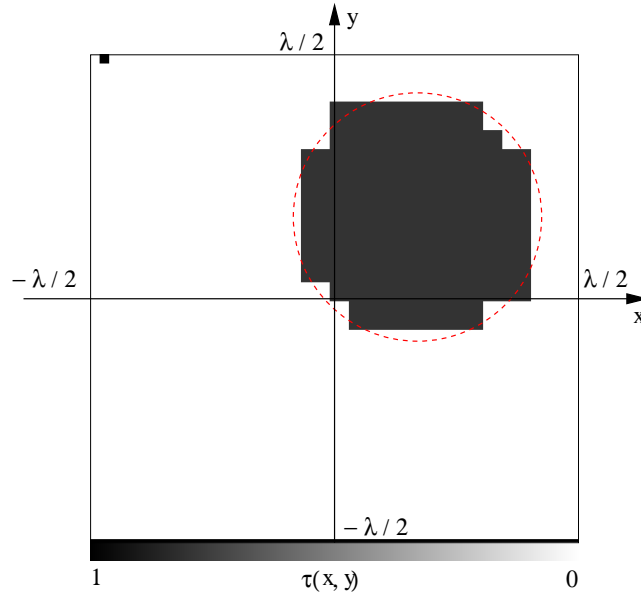


Figure 2. Choice of the optimal Δt . Reconstruction of a cylinder having radius $\lambda/2$ with $\Delta t = \Delta t_{opt,(s)}$.

Starting from the information achieved in s th reconstruction step, $R_{(s+1)}$ is then defined as the area where the unknown scatterer has been detected: towards this end, the barycenter $(X_{C_{(s+1)}}, Y_{C_{(s+1)}})$ and the side $L_{(s+1)}$ of the $(s+1)$ th region of interest have to be computed at each step according to the IMSA formulation [4]. Thus, $R_{(s+1)}$ is discretized in N_{IMSA} sub-domains and a new minimization process is considered in order to achieve an upgraded profile of the problem unknown $\tau(\underline{r})$.

The iterative multi-resolution procedure is repeated until the achieved reconstruction becomes stationary ($s = s_{opt}$) or a maximum number of steps ($s = S_{max}$) is reached.

3. NUMERICAL RESULTS

The first result deals with the choice of the proper time-step Δt , which is used inside the numerical Hamilton-Jacobi equation to perform the finite difference. The time-step represents a key parameter for the Level-Set-based optimization because it is concerned with the update of the Level Set function. A wrong choice of Δt could involve too fast an evolution of the Level Set (i.e., the real solution is never achieved) or, on the contrary, useless computations.

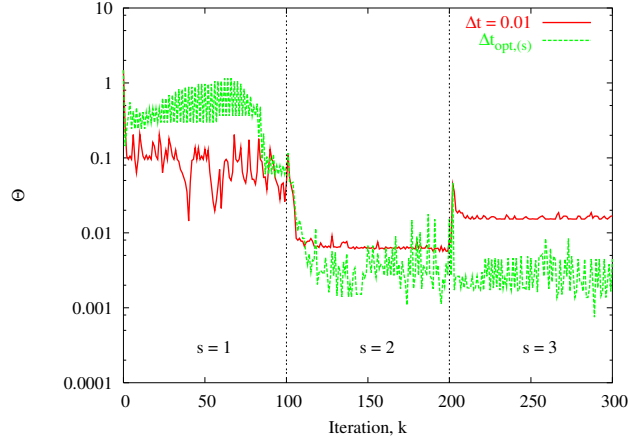


Figure 3. Choice of the optimal Δt . Comparison between the behavior of the fitness function ($\Delta t = 0.01$ —, $\Delta t = \Delta t_{opt,(s)}$ ···).

In order to perform the choice of Δt when using the multi-resolution approach, a known scenario has been considered. In particular, a cylindrical object of radius $\lambda/4$ [whose barycenter is located at $(\lambda/6, \lambda/6)$] is set within a square investigation domain D_I of side $l_{D_I} = \lambda$ [2]. The scenario is illuminated by means of $V = 10$ TM plane-wave sources and the data are collected in $M(v) = 10$ measurement points (D_O) located on a circumference of radius $\rho = \lambda$ centered at the origin of the Cartesian coordinate system. The working frequency of the electromagnetic sources is set to $f = 10$ [GHz].

As far as the electromagnetic properties are concerned, the known dielectric relative permittivity of the unknown non-dissipative object is $\epsilon_C = 1.8$.

A first trial has been performed by using a constant value for Δt during the multi-step procedure. The optimal value $\Delta t = \Delta t_{opt} = 10^{-2}$ has been chosen after several numerical experiments performed with a single-resolution technique. The results achieved have been compared with those given by a variable time-step related to the cell side $l_{(i)}$ ($i = 1, \dots, I_R$), according to $\Delta t = \Delta t_{opt,(s)} = C \cdot l_{(i)}$, with $C = \Delta t_{opt}/l'$, where $l' = 1.43 \cdot 10^{-2}\lambda$ is the cell side used in [2] for $\Delta t = \Delta t_{opt} = 10^{-2}$. The reconstructions obtained at step $s_{opt} = 3$ with $\Delta t = 0.01$ and $\Delta t = \Delta t_{opt,(s)}$ are shown in Figs. 1 and 2, respectively. The multi-resolution processes have been carried out with $N_{IMSA} = 81$ and a cell side $l_{(s_{opt})} \cong \lambda/14$ has been used at the latest step s_{opt} . Moreover, no stopping criterion has been employed for the optimization and the final results have been achieved by imposing $K_{max} = 100$. In order to avoid the inverse crime, the discretization in the direct problem is $N_d = 2601$.

When using $\Delta t = \Delta t_{opt,(s)}$ (Fig. 2, where the actual scatterer is indicated by the dotted line), the reconstruction shows a better estimation of the shape of the cylinder, while a good localization was achieved in both cases. Choosing $\Delta t = \Delta t_{opt,(s)}$ seems to be the best option, since a lower value of the fitness function (5) can be obtained: in Fig. 3 the behavior of the normalized error is shown with respect to $k = \sum_{i=1}^{I_R} k_i$.

In order to perform a numerical validation of the IMSA Level Set, the same scenario has been considered with noisy data. The scattered field collected in the observation domain D_O has been corrupted by an additive Gaussian noise characterized by different signal-to-noise ratios (SNRs). According to the criterion suggested in [7][8] and taking into account the amount of a-priori information in the problem at hand, the resolution inside $R_{(s)}$ has been increased by using $N_{IMSA} = 225$. The parameters employed for the convergence checks explained in Section 2 are $J_{\mathfrak{S}} = J_{\tau} = 10$, $\gamma_{\mathfrak{S}} = 1 \cdot 10^{-5}$, and $\gamma_{\tau} = 1$ ($K_{max} = 100$). In this case, the Level-Set-based minimization is stopped only by the criterion concerned with the normalized error.

The result of multi-resolution approach for $SNR = 5$ [dB] is shown in Fig. 4 ($s_{opt} = 2$): a good accuracy (i.e., localization and shape reconstruction) has been achieved, although the size of the cylinder is underestimated.

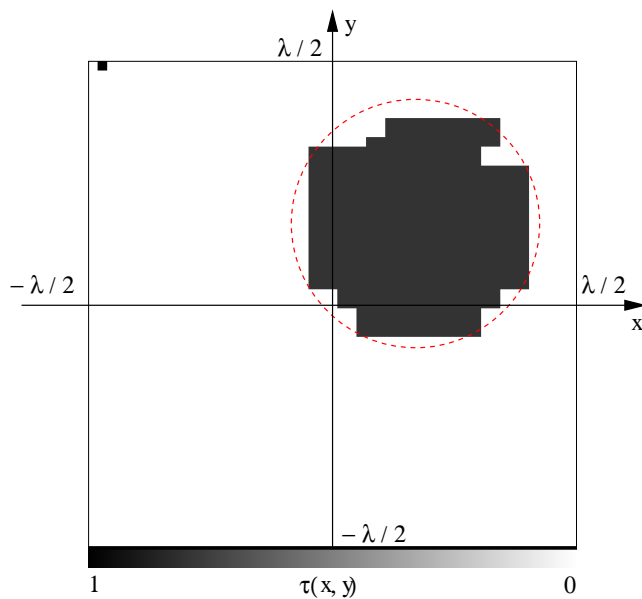


Figure 4. Reconstruction of a cylinder having radius $\lambda/2$ using the IMSA ($l_{D_I} = \lambda$, $SNR = 5[dB]$).

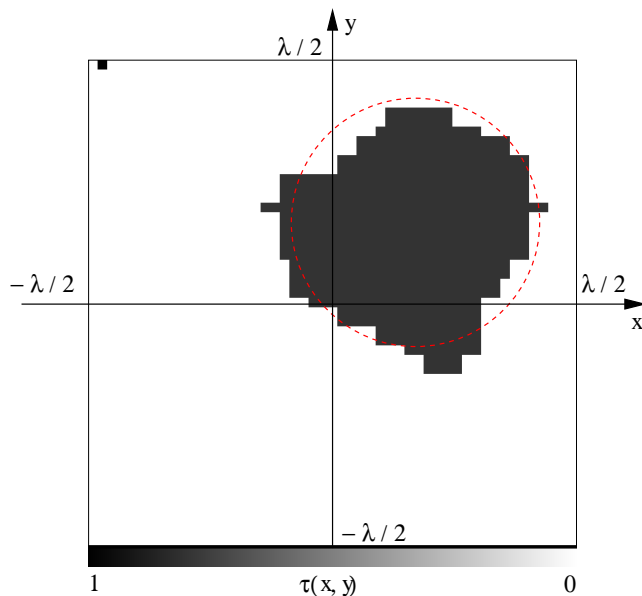


Figure 5. Reconstruction of a cylinder having radius $\lambda/2$ using the BARE approach ($l_{D_I} = \lambda$, $SNR = 5[dB]$).

The result of Fig. 4 has been compared with the single-resolution reconstruction. In particular, let us call “BARE approach” the Level-Set-based minimization with the cell side $l_{BARE} = l_{(s_{opt})}$. The number of views V and measurement points $M(v)$ is the same as used in multi-resolution approach, whereas the time-step Δt is computed as $\Delta t = C \cdot l_{BARE}$. For the adopted scenario, $l_{(s_{opt})} \cong \lambda/31$ and therefore $N_{BARE} = 961$. As far as the stopping criterion is concerned, the BARE approach employs the same parameters as IMSA, but $K_{max} = 300$. The result given by the single-resolution approach is shown in Fig. 5. The object is correctly localized but the shape is better estimated when using the IMSA.

A different scenario is now considered. The object to be retrieved is always a circular cylinder of radius $\lambda/4$ set within an investigation domain of side 2λ ($\rho = 2\lambda$) and centered in $(14\lambda/30, -14\lambda/30)$. This configuration should be considered as more critical to be inverted, since the object is smaller than in the previous scenario and consequently the discretization grid for the first step of IMSA has to be chosen carefully.

Again, the guidelines suggested in [7][8] have been followed in order to determine the optimal N_{IMSA} . In particular, let

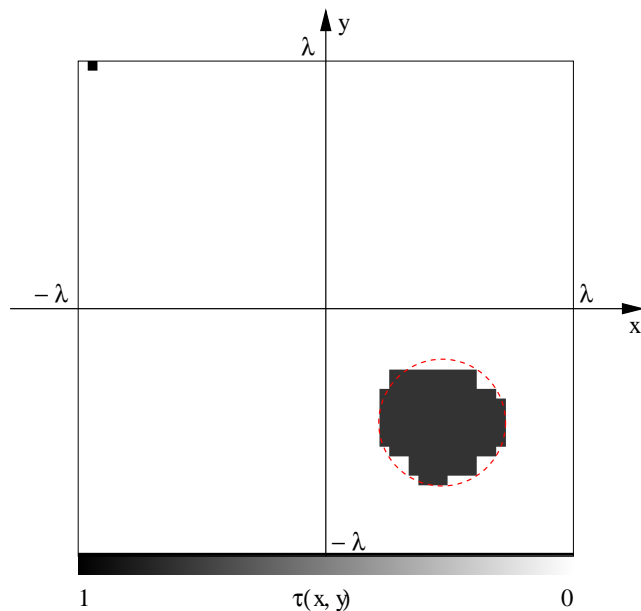


Figure 6. Reconstruction of a cylinder having radius $\lambda/2$ using the IMSA ($l_{D_I} = 2\lambda$, $SNR = 5[\text{dB}]$).

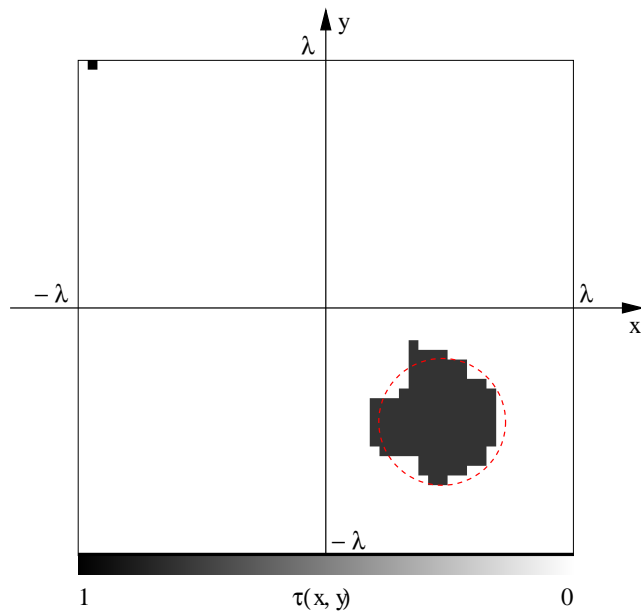


Figure 7. Reconstruction of a cylinder having radius $\lambda/2$ using the BARE approach ($l_{D_I} = 2\lambda$, $SNR = 5[\text{dB}]$).

us choose $M(v) = 20$, $V = 20$, and $N_{IMSA} = 169$ (i.e., the cell side at first step of IMSA is equal to $l_{(s=1)} = \frac{\lambda}{6.5}$). As far as the stopping criterion is concerned, the following parameters have been considered: $J_{\mathfrak{S}} = J_{\tau} = 50$, $\gamma_{\mathfrak{S}} = 2 \cdot 10^{-1}$, and $\gamma_{\tau} = 2 \cdot 10^{-2}$ ($K_{max} = 500$).

The result of the inversion of noisy data ($SNR = 5[\text{dB}]$) achieved by the multi-resolution procedure at step $s = 3$ ($l_{(s_{opt})} = \lambda/23$) is reported in Fig. 6. A better shape detection is provided with respect to the result of BARE approach with $N_{BARE} = 2209$ (Fig. 7).

As far as the behavior of the error (Fig. 8) is concerned, a lower value of the cost function is reached by IMSA when the algorithms stop, although a greater number of iteration is needed. However, since the complexity of Level-Set-based optimization is about $\mathcal{O}(2 \times \mathcal{N}^3)$ at each iteration, with $\mathcal{N} \in \{N_{IMSA}, N_{BARE}\}$, the multi-resolution approach turns out to be less computationally expensive than the single-resolution method.

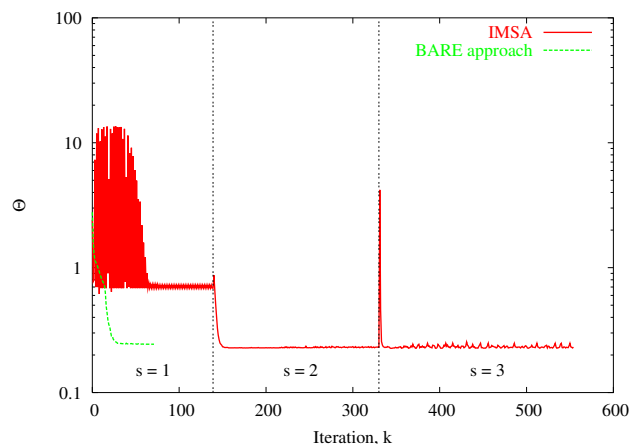


Figure 8. Comparison between the behavior of the fitness function (IMSA —, BARE ···).

4. CONCLUSION

In this work a preliminary analysis of the integration between the Iterative Multi-Scaling Approach and the Level-Set-based method has been proposed. The results obtained appear to confirm the feasibility as well as the robustness of the integration, since a higher resolution of the object under test is achieved without increasing the computational complexity of the inversion procedure and allowing a non-negligible time-saving.

REFERENCES

- [1] O. M. Bucci and G. Franceschetti, "On the spatial bandwidth of scattered fields," *IEEE Trans. Antennas Propagat.*, vol. 35, no. 12, pp. 1445-1455, 1987.
- [2] A. Litman, D. Lesselier, and F. Santosa, "Reconstruction of a two-dimensional binary obstacle by controlled evolution of a level-set", *Inverse Problems*, 14, 1998, pp. 685-706.
- [3] S. Caorsi, A. Massa, and M. Pastorino, "A crack identification microwave procedure based on a genetic algorithm for nondestructive testing," *IEEE Trans. Antennas Propagat.*, vol. 49, pp. 1812-1820, 2001.
- [4] S. Caorsi, M. Donelli, D. Franceschini, and A. Massa, "A new methodology based on an iterative multiscaling for microwave imaging," *IEEE Trans. Microwave Theory Tech.*, vol. 51, no. 4, pp. 1162-1173, 2003.
- [5] F. Santosa, "A level-set approach for inverse problems involving obstacles," *ESAIM: COCV*, vol. 1, pp. 17-33, 1996.
- [6] O. Dorn and D. Lesselier, "Level set methods for inverse scattering", *Inverse Problems*, 22, 2006, pp. R67-R131.
- [7] O. M. Bucci and T. Isernia, "Electromagnetic inverse scattering: retrievable informations and measurement strategies," *Radio Sci.*, vol. 32, pp. 2123-2138, Nov.-Dec. 1997.
- [8] T. Isernia, V. Pascazio, and R. Pierri, "On the local minima in a tomographic imaging technique," *IEEE Trans. Antennas Propagat.*, vol. 39, no. 7, pp. 1596-1607, July 2001.
- [9] S. Caorsi, M. Donelli, and A. Massa, "Detection, location and imaging of multiple scatterers by means of the iterative multiscaling method," *IEEE Trans. Microwave Theory Techn.*, vol. 52, pp. 1217-1228, 2004.